

Building on the WLF/Free Volume Framework: Utilization of the Coupling Model in the Relaxation Dynamics of the Gelatin/Cosolute System

Stefan Kasapis*

Department of Chemistry, National University of Singapore, Block S3, Level 6, Science Drive 4,
Singapore 117543

Received February 28, 2006

The onset of softening in the glass transition dispersion of the gelatin/cosolute system at 78% solids was examined using the stress relaxation modulus and dynamic oscillatory data on shear. Measurements were made between 5 and $-70\text{ }^{\circ}\text{C}$, and isothermal runs were reduced to a master curve covering 21 orders of magnitude in the time domain. The sharpness with which the mechanical properties of our system changed with temperature was reflected in the shift factor a_T used to pinpoint the glass transition temperature (T_g). The prevalent analytical framework traditionally employed to follow the transition from the rubbery to glasslike consistency in biomaterials is that of the free volume theory in conjunction with the WLF equation. Increasingly, the combined WLF/free volume approach is challenged by the coupling model, which is able to provide additional insights into the physics of intermolecular interactions in synthetic materials at the vicinity of T_g . The model in the form of the Kohlrausch–Williams–Watts function described well the spectral shape of the local segmental motions of gelatin/cosolute at T_g . The analysis provided the intermolecular interaction constant and apparent relaxation time, parameters which depend on chemical structure. Results appear to be encouraging for further explorations of the dynamics of densely packed biomaterials at the glass transition region.

Introduction

It is interesting to observe the evolution of the science of the glassy phenomena by following its development to a highly specialized subject, especially one that cuts across several conventional fields.¹ From the onset, scientific understanding of glassy systems evolved around the fundamental question of the thermodynamic or kinetic nature of vitrification.² The temperature at which the sample exhibits glassy behavior has been known as T_g , but it is not as well-defined as, for example, the melting point (T_m), since it was observed that the process of vitrification may take place over a wide range of temperatures (glass transition region).^{3,4} It is now well-known that this “second-order transition” is not a thermodynamic process at equilibrium but, rather, a kinetic process originating from restrictions in the rates of internal adjustments or intermolecular mobility due to temperature, mechanical stress, or hydrodynamic pressure variations. Glasslike consistency is also observed by changing the experimental time scale or frequency of observation.^{5,6}

It is quite remarkable that the free energy, volume, or enthalpy relaxations associated with glassy systems are universal phenomena and allow utilization of a wide range of techniques with a micro- or macrostructural nature, e.g., positron annihilation lifetime spectroscopy, calorimetry, and dilatometry. Thus, a common reference can be made to quantities such as “free volume” or “configurational entropy” to obtain results, which have physical meaning for several approaches. In synthetic polymer science, the approach used extensively to develop a mechanistic understanding of the mechanical glass transition is based mainly on the concept of free volume.⁷ Free volume is a

useful semiquantitative, although somewhat poorly defined, concept closely related to the hole theory of liquids. The total volume per mole, u , is pictured as the sum of the free volume, u_f , and an occupied volume, u_o . Ferry takes u_o as including not only the van der Waals radii but also the volume associated with local vibrational motion of atoms.⁸ The free volume is therefore that extra volume required for larger-scale vibrational motions than those found between consecutive atoms of the same chain. Flexing over several atoms, that is, transverse stringlike vibrations of a chain rather than longitudinal or rotational vibrations, will obviously require extra room.⁹ The free volume concept is popular partly because of its being intuitively appealing. Often (but not invariably), it is able to explain observed trends correctly in synthetic polymers, low molecular weight organic liquids, and inorganic compounds, and is easy for workers in materials science coming from many different backgrounds.^{10–12}

Recently, there has been a certain opposition in the use of free volume, since in physics of the densely packed systems, “intermolecular interactions determine volume but not vice versa”.¹³ Thus, interactions appear to be more fundamental and the ultimate determining factor of molecular dynamics in these materials. A new concept, “the coupling model”, has been put forward to overcome the oversimplification associated with the application of free volume to the entirety of the glass transition region.^{14–16} Despite the postulates of the free volume theory that vitrification phenomena are not associated with specific details of chemical structure, it is likely that, in order to follow the development of properties within the (broad) transition region, the theory has been unable to pinpoint the intermolecular cooperative dynamics responsible for the diffusional mobility around the glass transition temperature. The purpose of the present investigation is to discuss the two concepts in the

* Email: chmsk@nus.edu.sg. Fax: +65 6775 7895. Tel: +65 6516 4834.

Table 1. Data on the Physicochemical Characterization of the Gelatin Sample

characteristic	gelatin (PC2)
bloom ^a (g)	189
isoelectric point (pI)	4.5
% moisture (wwb)	9.2
calcium (ppm)	80
sulfate (%)	<0.1
chloride (%)	0.16
phosphate (ppm)	53
M_n^b	67 200
M. Wt. > 10 ⁶ kD	7.81
M. Wt. > 540 kD	8.37
tetra + penta	7.53
γ	7.58
β	15.34
α	23.94
subunits 1	10.45
subunits 2	7.86
subunits 3	3.40
subunits 4	7.88

^a Bloom is the weight in grams required to push a piston of strictly defined shape 4 mm into a gelatin gel matured for 16–18 h at 10 °C.

^b The α , β , and γ fractions of gelatin are well-characterized and monodisperse with characteristic masses. The latter two are, respectively, a dimer and a trimer of the α fraction. The tetra and penta are higher order but less well defined fractions. The low molecular weight side of the GPC spectrum is divided arbitrarily into four different fractions of subunits. The percent weight of the GPC spectrum in each of the 10 molecular mass classes is quoted.

vitrification of the gelatin/cosolute system and in conjunction with the published literature on the glass dispersion of amorphous polymers and biomaterials.

Experimental Section

Materials. The gelatin sample came in the form of a fine powder, and it was prepared especially for research from Sanofi Bio-Industries, Baupré, Carentan, France. It was the second extract (PC2) from a single batch of cowhide produced by alkaline hydrolysis of collagen (type B). In comparison to the acidic process on pigskin, cowhides require longer and more drastic lime treatment before extraction, as the skins are much older. In this case, the treatment may last several months, and the long soak converts many of the basic side chains into acidic groups, thus reducing considerably the resultant gelatin's isoelectric point (pI = 4.5 in our case) due to the amidolysis of asparagine and glutamine amino acid residues. Table 1 reproduces analytical characteristics of the sample, which were determined by the manufacturer. The isoelectric point was measured by completely deionizing the sample on a bed of ion-exchanged resin and then measuring the pH of the eluant. Gel permeation chromatography was used to identify the number average molecular weight (M_n) of the sample and the percent weight of ten molecular mass classes. Pullulan with a number average molecular weight ranging from 6 to 788 kD was used as a standard. The bloom value is proportional to the elastic modulus of the gelatin gel and decreases with decreasing M_n . Moisture content of the gelatin powder was accounted in the final composition of the protein in the experimental samples.

The glucose syrup was supplied by Cerestar, Trafford Park, Manchester, U.K. The dextrose equivalent (d.e. gives the content of reducing endgroups relative to glucose as 100) of the sample is 42, and it contains 18% water. The water content of the glucose syrup was considered in calculating the composition of samples, and the glucose syrup content in this paper refers to dry solids. The material has been thoroughly characterized, and details of its composition have been published previously.¹⁷ Sucrose was AnalaR grade from Sigma-Aldrich Corp., St. Louis, MO.

Methods. Gelatin samples were prepared by soaking the granules in distilled water overnight and then heating to 60 °C. High-solid materials were made by adding appropriate amounts of glucose syrup and sucrose (1:1) preheated to 60 °C to the gelatin solution, thus producing systems with the required composition. Stress relaxation and dynamic oscillation routines have been used to demonstrate the formation of structures with distinct mechanical properties occurring with changing temperature. The analysis provided readings of the time-dependent change in stress following a step change in strain (stress relaxation modulus, $G(t) = \sigma(t)/\epsilon$).¹⁸ In addition, preparations were subjected to an alternating strain on shear, and the stress was simultaneously measured, thus providing values of the shear storage modulus (G'), which is the elastic component of the network, and the shear loss modulus (G'' , viscous component).

Measurements were performed with the Advanced Rheometrics Expansion System (ARES), which is a controlled strain rheometer (Rheometric Scientific, Piscataway, NJ). ARES has an air-lubricated and essentially noncompliant force rebalance transducer with a torque range between 0.02 and 2000 g/cm. Nevertheless, particular care was taken to establish that any inherent machine compliance was insufficient to significantly offset measured values from the high-modulus glass systems. This was achieved by progressive adjustment of geometry settings while measuring samples of known intermediate and high modulus, namely, polydimethylsiloxane (PDMS) at 30 °C ($G_c = 2.5 \times 10^4$ Pa) and ice at -20 °C ($G' = 10^9$ Pa).¹⁹ Thus, maximum plate diameter (10 mm) and minimum measuring gap (3 mm) between the two parallel plates consistent with accurate results could be established. In doing so, triplicate runs of different preparations reproduced readily the rubber-to-glass transition within a 3% error margin as a function of temperature or time scale of measurement.

For precise control of sample temperature, an air convection oven was used which has a dual element heater/cooler with counter-rotating air flow covering a wide temperature range (between 130 °C and -70 °C). This allowed monitoring of the viscoelastic properties of our preparations from the rubbery and the glass transition to the glassy state. Samples were loaded onto the preheated platen of the rheometer (50 °C), their exposed edges were covered with a silicone fluid from BDH (100 cs) to minimize water loss, and they were cooled to subzero temperatures (-70 °C) at a rate of 1 °C/min. The silicon fluid was of sufficiently low molecular weight to remain liquidlike at subzero temperatures. Cooling was followed by a heating scan at 1 °C/min to temperatures above 0 °C. Throughout the experimental temperature range, the frequency of oscillation was kept at 1 rad/s.

Overall, the experimental temperature range allowed access to molecular motions that cover the glassy state, the softening dispersion (glass transition region), and "rubbery plateau". This led to combined master curves of shear modulus (G' and G'') and their ratio, $\tan \delta$ (G''/G') versus temperature within the linear viscoelastic region. It was noted that the cooling and heating traces of shear modulus were superposable, which is a characteristic of the rheological glass transition. Isothermal time patterns of transient nature ($G(t)$) were obtained at fixed temperature intervals of 5 °C. Data were recorded by allowing the stress to relax for 17 min at each temperature. In this type of measurements, the instantaneous strain varied approximately from 0.000712% in the glassy state and 0.01% in the glass transition region to 1.0% in the rubbery plateau in order to accommodate the spectacular changes in the measured stiffness of the sample. As in the case of dynamic oscillatory experiments, three runs were recorded, and the average of essentially overlapping traces is reported.

Results and Discussion

Experimental Observations of the Relaxation Behavior of the Gelatin/Cosolute System. In general, the molecular processes of real viscoelastic materials as a function of temperature or time of observation are too complex to be described directly by a single model. As the material structure becomes more

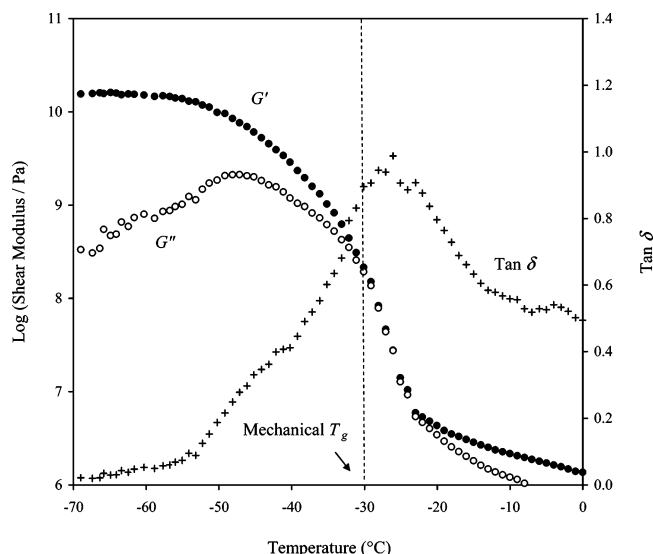


Figure 1. Temperature variation of shear moduli and $\tan \delta$ of a system containing 15% gelatin, 31.5% glucose syrup, and 31.5% sucrose, with the dashed line indicating the mechanical T_g (scan rate, 1 °C/min; frequency, 1 rad/s; strain, 0.000712 to 2%).

complex, so the number of relaxation processes at different experimental conditions contributing to the overall mechanical properties increases. Figure 1 reproduces the relaxation transition of a system containing 15% gelatin, 31.5% glucose syrup, and 31.5% sucrose, as a function of changing temperature. We composed the mixture as it was in order to avoid ice formation or sucrose crystallization, thus focusing efforts on vitrification phenomena. Initially, the transition was studied using the shear moduli of storage and loss modulus, and the derived damping factor ($\tan \delta = G''/G'$) due to the fundamental and applied importance of this phenomenon lying partially in the associated changes of these mechanical properties.

At the high-temperature end (above -20 °C), the observed pattern of response is qualitatively similar to that of a rubbery plateau, i.e., $G' > G''$, with little frequency dependence of either modulus. The magnitude of the pseudo-equilibrium storage modulus in Figure 1 is an order of magnitude higher than for the aqueous protein preparations with comparable molecular characteristics.²⁰ Recently, TEM images made a case for phase-separated gelatin and cosolute-rich domains in a high-solid environment,²¹ and this should be the origin of the reinforced network strength in the present system ($G' = 10^{6.13}$ at 0 °C). This paper is not going to dwell upon the effect of temperature and concentration on the gelation characteristics and network morphology of the aqueous gelatin preparations (typically between 0.5% and 30% protein solids), which have been discussed extensively in the literature.^{22,23}

On further cooling (below -20 °C), values of both moduli increase steeply, leading to convergent lines and $\tan \delta$ estimates of about 1. The spectacular development in viscoelasticity is thermally reversible, and it is governed by configurational vibrations of segments of the molecule, which are shorter than the distance between cross-links or points of entanglement. Attempts have been made to associate the entirety of this transition with a particular molecular movement, but it is clear that the polydisperse nature of biomacromolecules will produce a composite response comprising an array of minute step changes.¹³ The second part of this work will address directly the issues associated with the breadth of viscoelastic dispersions in an effort to identify the modality of molecular motions contributing to the time dependence of the glass transition temperature.

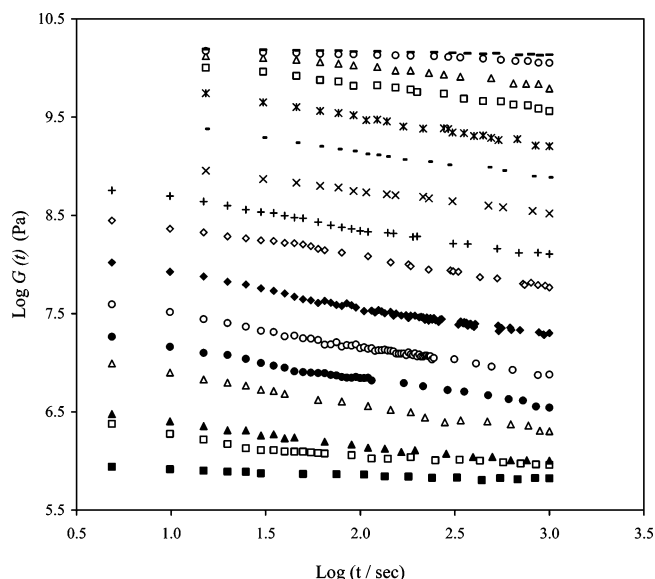


Figure 2. Variation of the stress relaxation modulus at fixed temperatures for the sample in Figure 1. Bottom curve is taken at 5 °C (■); other curves successively upward: 0 (□); -5 (▲); -10 (△); -15 (●); -20 (○); -25 (◆); -30 (◇); -35 (+); -40 (×); -45 (−); -50 (*); -55 (□); -60 (△); -65 (○); -70 (−) °C.

Once more, the elastic component of the network dominates throughout the lower range of experimental temperatures (below -40 °C) in Figure 1. Such behavior has been reported for synthetic polymer systems and corresponds to the glassy state at which molecular movement from one lattice site to another requires overcoming a considerable energy barrier.²⁴ Completion of the sigmoidal modulus–temperature curve is accompanied by a large drop in the values of $\tan \delta$ (~ 0.02 at -70 °C), further emphasizing the characteristic solidlike behavior of the “foot” region of the viscoelastic spectrum. Although not previously seen for a biopolymer in a high-water system, such behavior can be achieved in a high cosolute environment. A mixture of sucrose and glucose syrup (63% total) was added to 15% gelatin in order to prevent ice formation at subzero temperatures. The present mechanical profile, however, is due to the protein vitrification, since the direct low-viscosity solution to glass transformation of the sucrose/glucose syrup mixture is quite distinct.²⁵ Thus, it is well-known in the literature that sugars do not exhibit the mechanical rubber-to-glass transformation shown for gelatin in Figure 1. Furthermore, vitrification of a 78% sugar solution will produce T_g values of about -48 °C for the glucose syrup of this investigation (d.e. = 42)⁵² and -51 °C for sucrose,²⁶ as opposed to the higher T_g of our gelatin sample (-30 °C in the discussion of the second part of this work).

The preceding section made a start in discussing the structural properties of gelatin/cosolute as a function of the experimentally accessible temperature range always at the same time interval (i.e., oscillatory frequency of 1 rad/s). From a fundamental point of view, the intention should be to generate complementary understanding as a function of time, thus achieving a far more instructive separation of the two variables. The latter was pursued by implementing a series of time runs at fixed temperatures covering the range of 5 to -70 °C and monitoring the stress-relaxation modulus shown in Figure 2. From the relations among the viscoelastic functions, it follows that any modulus function can be used to obtain isothermal data, and indeed, the real and imaginary parts of the complex shear modulus, $|G^*| = (G'^2 + G''^2)^{1/2}$, have been applied widely to synthetic and biomaterial vitrification.^{27–29} The present inves-

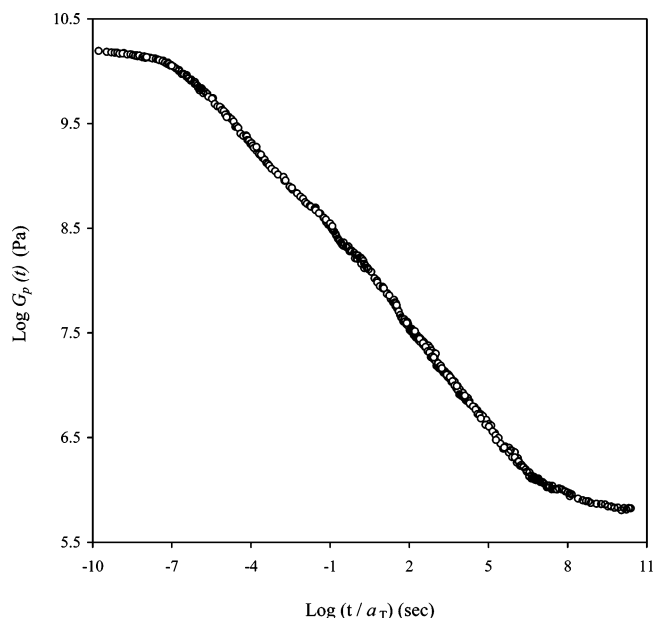


Figure 3. Master curve of stress relaxation modulus for the preparation in Figure 1 reduced to $-25\text{ }^{\circ}\text{C}$ and plotted logarithmically against reduced time (t/a_T) utilizing the experimental isothermal runs of Figure 2.

tigation opted to utilize measurements of the modulus $G(t)$ at constant deformation in order to expedite estimation of the relaxation time within the temperature domain of devitrification. True, numerical techniques are available to obtain $G(t)$ from G' and G'' ,³⁰ but the Fourier transforms involved may discourage workers from doing so.

Figure 3 illustrates the composite (or master) curve produced by an empirical superposition of the data obtained at different temperatures in Figure 2. Only horizontal shifts along the logarithmic time axis were implemented, which centered around the reference temperature of $-25\text{ }^{\circ}\text{C}$ (T_0). The arbitrary choice of reference temperature is inconsequential as long as it is confined within the glass transition region. The scheme of developing a composite curve is known as the method of reduced variables or time-temperature superposition (TTS), and through the years, it was applied to a plethora of measurements.^{31,32} Good matching of the shapes of adjacent curves has been achieved presently, a criterion which is critical for the applicability of the method of reduced variables. The transition zone from a "rubbery" state at long times ($>10^8\text{ s}$) to a "glassy" state at short times ($<10^{-7}\text{ s}$) is clearly discernible, thus demarcating a spectacular dependence of stress-relaxation modulus on time. Values of $G_p(t)$ do not change much with time in the rubbery and glassy states, but they do rapidly in the glass transition ($10^6\text{--}10^{10}\text{ Pa}$). In the following, we shall attempt to develop an explicit discussion of the nature of molecular processes based on the behavior of the gelatin/cosolute sample over an extended time scale at various reference temperatures.

Modeling the Relaxation Behavior of the Gelatin/Cosolute System using the Combined WLF/Free Volume Framework. To move from a qualitative description to quantitative treatment, use is made of the shift factor, a_T , which was used in the reduction of data in Figure 2 by plotting in Figure 3 as follows:

$$G_p(t) = G(t) T_0 \rho_0 / T \rho \quad \text{vs} \quad t/a_T \quad (1)$$

where $G_p(t)$ is the reduced stress-relaxation modulus and ρ_0 is the density of the material at T_0 . It should be noted that, in the case of dynamic oscillation data, this fundamental descriptor

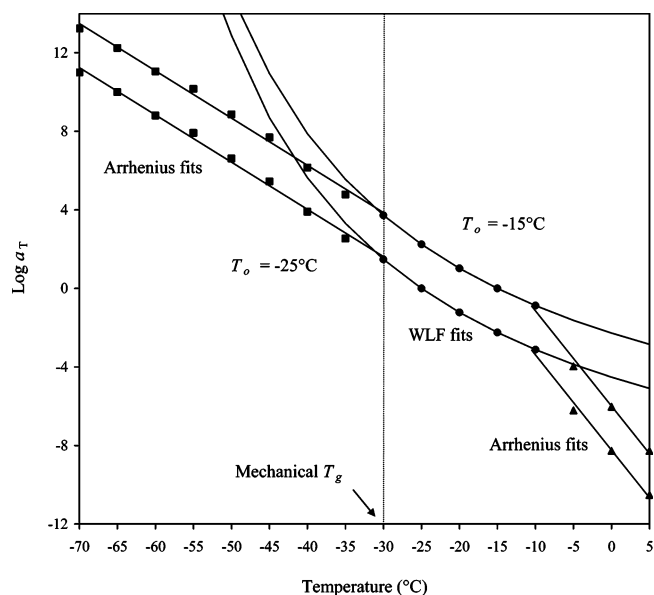


Figure 4. Logarithm of the reduction factor, a_T , for the sample in Figure 1 plotted against temperature from the data of the master curve in Figure 3. Reference temperatures, mechanistic modeling, and the mechanical glass transition temperature are also shown.

(i.e., the shift factor, a_T) of the temperature dependence is plotted as ωa_T , where ω is the frequency of oscillation. In practice, satisfactory matching of adjacent curves is achieved without the vertical shift of the temperature and density factors, since their logarithms are relatively small compared to the rapid changes in viscoelastic functions with experimental temperature.³³

Figure 4 reproduces the effect of temperature on the molecular mobility of the gelatin/cosolute system from the glassy state to the rubbery plateau. Clearly, the set of horizontal shift factors yields a plot that is not a straight line in its entirety, so the temperature dependence of a_T is not a simple exponential function. Two discontinuities appear at -10 and $-30\text{ }^{\circ}\text{C}$, creating three $\log a_T$ vs temperature curves, which fan out but do not superpose onto a single line. Qualitatively, it is known that molecular motions are greatly inhibited as the biopolymer solution is cooled through the gel to the glassy state, but the question is of identifying a description which is close to a molecular interpretation of the observed phenomena.

It was verified that, above $-10\text{ }^{\circ}\text{C}$ and below $-30\text{ }^{\circ}\text{C}$, $\log a_T$ is a linear function of reciprocal absolute temperature; these results are plotted against degrees Celsius in Figure 4. By analogy with the theory of rate processes, the following expression will emerge for the interplay of relaxation time and temperature:³⁴

$$\log a_T = \frac{E_a}{2.303R} \left(\frac{1}{T} - \frac{1}{T_0} \right) \quad (2)$$

where R is the gas constant. Equation 2 relates to a constant activation energy of a particular mechanism (E_a) within the relevant temperature range, which is obtained from the gradient of a linear relationship between $\log a_T$ and $1/T$. It appears that the amount of shift on the logarithmic scale being, of course, equal to $\log a_T$ is followed by the modified Arrhenius relationship in the rubbery plateau and the glassy state. At the intermediate regime, however, a curve is obtained in accordance with the analysis of the aforementioned discussion, which argues strongly for a non-Arrhenius process.

The inability of the predictions of the reaction rate theory to hold at the glass transition region has been the subject of considerable debate, and it was found that the Williams, Landel, and Ferry equation (WLF) could better describe the relaxation processes derived from transient, dynamic, or viscosity measurements of synthetic polymers.³⁵ In the case of the stress-relaxation modulus, the WLF equation would be

$$\log a_T = \log[G(t)(T)/G(t)(T_o)] = - \frac{(B/2.303f_o)(T - T_o)}{(f_o/\alpha_f) + T - T_o} \quad (3)$$

At any reference temperature, T_o , eq 3 can include two constants which relate to the free volume theory as follows:

$$C_1^o = B/2.303f_o$$

and

$$C_2^o = f_o/\alpha_f \quad (4)$$

where the fractional free volume, f_o , is the ratio of free to total volume of the molecule, α_f is the thermal expansion coefficient, and B is usually set to 1.

Clearly, the analysis amounts to more than curve-fitting, since it defines at -30°C in Figure 4 a turning point where large configurational vibrations requiring free volume in the glass transition region cease to be of overriding importance. At lower temperatures, the need to overcome an energetic barrier for the occurrence of local rearrangements from one state to the other becomes of primary importance according to eq 2. The approach affords a fundamental definition of the mechanical glass transition temperature for the gelatin/cosolute system. This is an improvement on several empirical indices of the mechanical T_g , which recorded an array of discontinuities in the slope of storage or loss modulus traces and large peaks in the damping factor, $\tan \delta$.^{36–39} In the absence of a fundamental criterion, however, it seems barely credible to pinpoint glassy phenomena or any other molecular events (thermal relaxation, molecular degradation, etc.) to empirical indices of pictorial rheology. Nonetheless, the glass transition temperature can be identified in terms of features of the molecular vitrification of gelatin discussed presently.

Interpretation of results in terms of the framework of the preceding paragraph yields a value of mechanical T_g (-30°C) which coincides with the completion of the glass transition region upon cooling in Figure 1. Within the limits of the transition region, eq 3 holds for any reference temperature (including the T_g), and an algorithm of simultaneous equations can be devised to determine parameters related to the glassy characteristics of a polymer⁴⁰

$$\begin{aligned} C_1^o &= C_1^g C_2^g / (C_2^g + T_o - T_g) \\ C_2^o &= C_2^g + T_o - T_g \end{aligned} \quad (5)$$

With eq 5, reduction of the gelatin/cosolute data produces free volume indicators, which are congruent with those for diluted synthetic polymers:³³ at the reference temperature, $T_o = -25^\circ\text{C}$, $C_1^o = 13.91$, $C_2^o = 52^\circ$, $f_o = 0.031$; and at the glass transition temperature, $T_g = -30^\circ\text{C}$, $C_1^g = 14.47$, $C_2^g = 50^\circ$, $f_g = 0.030$; $\alpha_f = 6.0 \times 10^{-4} \text{ deg}^{-1}$.

Introducing the Stretched Exponential of Kohlrausch, Williams, and Watts to the Structural Relaxation of the Gelatin/Cosolute System. It is clear from the experimental data

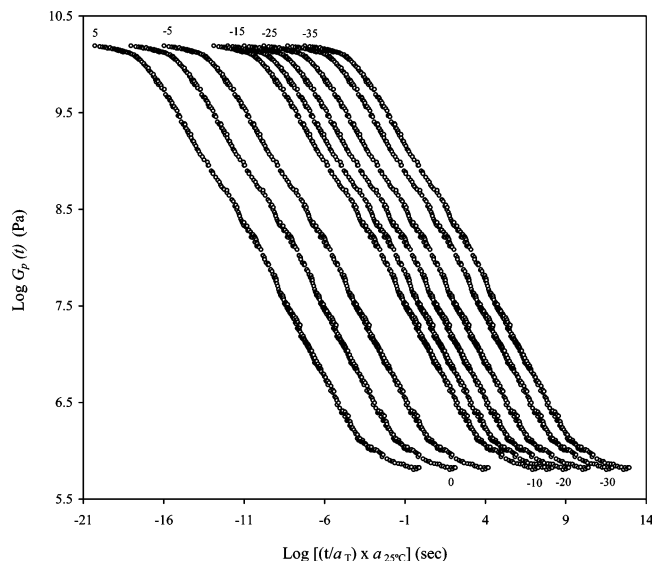


Figure 5. Master curves of stress relaxation modulus for the sample in Figure 1 plotted logarithmically against reduced time $[(t/a_T) \times a_{25^\circ\text{C}}]$ at the reference temperatures shown to the top and bottom of the individual traces.

and derived indicators in Figures 1–4 that the entirety of the glass transition region encompasses broad temperature and time domains which activate molecular motions emanating from residual amino acids (monomers) to polymeric segments of considerable length. It is further understood from Figure 5 that this composite of molecular dynamics exhibits a considerable time-scale shift with temperature. Thus, an extended spectral range of 35 orders of magnitude in the “time dispersion” was readily obtained by producing a series of isothermal master curves following appropriate data reductions within the rubber-to-glass transition. Vitrification phenomena shift to long times with decreasing reference temperature (from 5 to -35°C), but the spacing of the composite curves moves at a diminishing rate to longer times. The accelerated shift of the composite curves at the higher range of reference temperatures is due to the factor a_T changing more rapidly within the rubbery region (steep gradient of the modified Arrhenius fit between 5 and -10°C in Figure 4).

The gelatin/cosolute system appears to be thermorheologically simple (TS), implying that the major relaxation processes detected in Figure 5 have the same temperature dependence.⁴¹ This is not a universal observation, and indeed, thermorheological complexity (TC) has been reported on the superposition of viscoelastic functions in a number of amorphous materials and epoxy resins.^{14,42} It has been reported, however, that TC is more pronounced on low molecular weight materials, with the high molecular weight counterparts, as the gelatin fraction of the present investigation ($M_n = 67\,200$), exhibiting good superposition of mechanical data, hence leading to thermorheological simplicity.¹³

The analysis becomes more explicit, considering that even in thermorheologically simple systems the “softening dispersion” of the transition zone unveils a variety of mechanisms from the Gaussian submolecular motions of the extended Rouse model to the local segmental motions. At best, the former accounts for the long-time portion of the glass transition region.⁴³ Interesting physical phenomena, however, leading to the completion of vitrification with decreasing temperature, for example, are related to local segmental motions within the Gaussian submolecule. The motions, which were found to deviate from the predictions of the extended Rouse model, were first dealt

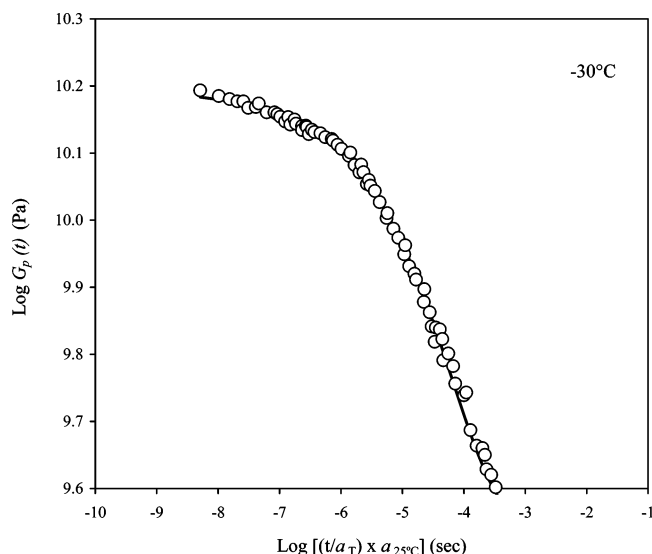


Figure 6. Short-time part of the stress-relaxation master curve for the sample in Figure 1 at the reference temperature of $-30\text{ }^{\circ}\text{C}$, with the solid line following the predictions of the stretched exponential KWW function.

with in the vitrification of synthetic polymers by Tobolsky and co-workers.⁴⁴ Subsequently, it became apparent that the relaxation pattern of these sub-Rouse and local segmental modes at high frequencies or short times of the glass transition region depended on the chemical structure of the macromolecule. For example, the contrasting behavior of the master curves of polystyrene and polyisobutylene constitute focal points of discussion in this respect.¹³

The nature of the local segmental motions is responsible for the glass transition temperature of an individual system, as monitored using several well-established techniques. In particular, the extent of interactions between neighboring segments relates to the distribution of relaxation times and can be followed by the so-called stretched exponential function of Kohlrausch, Williams, and Watts (KWW) in the time domain⁴⁵

$$\phi(t) = \exp[-(t/\tau)^\beta] \quad (6)$$

where τ is the relaxation time. The stretch exponent β can take values between 0 and 1.0, thus imparting a nonexponential character to the kinetics of structural relaxation of synthetic glasses. At the times appropriate for mechanical measurements, eq 6 recasts for the stress relaxation modulus of the present investigation as follows:⁴⁶

$$G(t) = (G_g - G_e) \exp[-(t/\tau)^{1-n}] + G_e \quad (7)$$

where G_g is the unrelaxed glassy modulus, G_e is the relaxed or equilibrium modulus of the local segmental motions, and t is the time after the application of a fixed strain. The coupling constant, n ($\beta = 1 - n$), ranges from 0 to 1.0 and reflects the intensity of interactions (coupling) between the primitive (underlying) relaxation and the physicochemical environment of the surrounding materials.

Figure 6 reproduces part of the stress-relaxation composite curve of the gelatin/cosolute sample, which constitutes the extreme short-time segment of the rubber-to-glass transition. With the KWW function of eq 7, data fit was attempted at the glass transition temperature ($T_g = -30\text{ }^{\circ}\text{C}$) where, besides the local segmental motions, other molecular mechanisms should have a minimal contribution to the viscoelastic spectrum. Equation 7 is applicable to relaxation patterns reflecting

segmental mobility, and therefore, values of experimental functions should fall within the range $G_g > G(t) > G_e$. Secondary (β) relaxations would be responsible for the region $G(t) > G_g$, whereas extended Rouse-like modes are expected to dominate at $G(t) < G_e$. In the present investigation, G_g and G_e are taken to be about 1.5×10^{10} and 3.5×10^9 Pa, respectively. This is in accordance with experience from the synthetic polymer research, e.g., results on unplasticized and plasticized poly(vinyl chloride), where the unrelaxed to relaxed modulus ratio is between 4.0 and 4.5, and modeling provides an adequate fit of the short-time section of the normalized spectrum.⁴⁷

As shown in Figure 6, the two-parameter KWW function follows well the progression of mechanical data reflecting the local segmental motion and returns τ and n values of $\sim 0.2 \times 10^{-4}$ s and 0.57 for the gelatin/cosolute preparation at $-30\text{ }^{\circ}\text{C}$ (the nonlinear analysis was carried out using Statistica v. 5.0, with the regression coefficient and regression loss of the estimated function being 0.998 and 0.018, respectively). The higher the value of n , the stronger the intermolecular coupling which originates from the chemical structure of the macromolecule and its surrounding environment. Experimentally, it was found that the n values of strongly interlinking or sterically interfering chains of synthetic materials range between 0.66 and 0.77 (poly(vinyl chloride), poly(methyl methacrylate), etc.).¹³ The present estimate of the coupling constant (0.57) is reasonable, in view of the nonaggregating nature of the gelatin molecule, and the recent finding that a decrease in the surface of contact between the protein and the polyhydroxyl cosolute is necessary to induce thermodynamically favorable conditions in the mixture.⁴⁸

Finally, we wish to utilize the present and previously reported results in an effort to discuss the issue of identifying the mechanical glass transition temperature based on an arbitrary predetermined relaxation time. In certain studies of amorphous and semicrystalline synthetics, this has been taken to be 100 s so that $T_g = T(\langle\tau\rangle = 100\text{ s})$.⁴⁹ In Figure 5, however, it is clear that the changing reference temperature results in a systematic shift of the softening dispersion in the time domain. Similar conclusions are reached presently utilizing earlier data of the gelatin/cosolute system,⁵⁰ through the treatment of superpositioned loss-modulus spectra, which are normalized at G''_{pmax} . Experiments were designed to yield reference temperatures (-8 , -11 , -14 , -20 , -23 , $-35\text{ }^{\circ}\text{C}$) encompassing T_g ($-16\text{ }^{\circ}\text{C}$ for PS1 gelatin/cosolute),⁵⁰ thus unveiling in Figure 7a a 6 orders of magnitude change in the G'' peak frequencies of glass-related motions (original treatment and depiction of data from ref 50).

Considering that the G'' peak frequencies are in the vicinity of the local segmental modes of the gelatin/cosolute mixture and converting them to an empirical relaxation time, we obtain Figure 7b, at which the inverse of absolute temperature on the abscissa creates an Arrhenius-type plot. Similar plotting is also depicted for the segmental relaxation behavior of a typical polybutadiene (PBD) rubber.⁴⁹ The relaxation map of both types of materials exhibits a considerable temperature dependence, and there is no fundamental basis in relating $\tau(T_g) = 100$ s or any hypothetical indicator to a glass point.

To circumvent the condition that makes the local segmental motions of various materials to associate with the same and arbitrary relaxation time, we opted to build on the temperature dependence of factor a_T shown in Figure 4. Regardless of the choice of reference temperature (e.g., -15 or $-25\text{ }^{\circ}\text{C}$), progression in viscoelasticity exhibits a discontinuity at $-30\text{ }^{\circ}\text{C}$ (the glass transition temperature in the present system), which

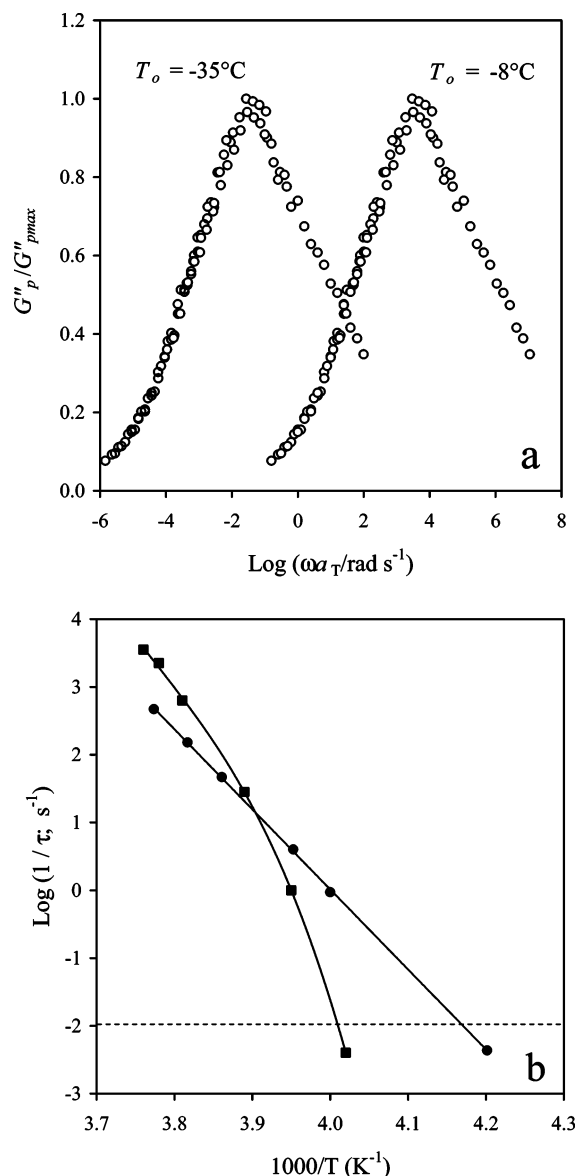


Figure 7. (a) Typical examples of normalized plots at the reference temperatures of -8 and -35 °C for loss modulus spectra plotted against reduced frequency of oscillation for 25% gelatin in the presence of 55% cosolute (original treatment and depiction of data from ref 50) and (b) Arrhenius plots of the inverse of the empirical relaxation time, derived from the G' peak frequencies, for the 25% gelatin plus 55% cosolute mixture (\bullet), and atactic 83% 1,2-polybutadiene (\blacksquare)⁴⁹ (dashed line indicates an apparent relaxation time of 100 s).

remains unaltered and dictates the local segmental motion. Data of the composite curve at T_g were used in the algorithm for calculating eq 7, thus providing an apparent relaxation time ($\tau \approx 0.2 \times 10^{-4}$ s) for the local segmental motions of the gelatin/cosolute system. This protocol is distinct from the assumed relationship between T_g and τ adopted earlier, and yet, the present measurement of the inhibited relaxation time is reasonable, since time frames between 10^{-12} and 10^{-15} s have been reported for the uncoupled (primitive) relaxation of local segmental motions within the range $0.1\text{--}5$ Å.⁵¹

Conclusions

In this paper, we have examined the application of the coupling model, in connection with the KWW function, to the

vitrification of the gelatin/cosolute system. This was obviated by the broad range of experimental times in stress-relaxation isotherms, which were superposed to yield master curves in the rubber-to-glass transition. The temperature dependence of factor a_T showed three distinct regions, which were utilized to pinpoint the mechanical glass transition temperature of the material. The glass point was correlated to the local segmental motions characterized by an apparent relaxation time and an interaction (coupling) constant. These are important characteristics of molecular mobility that may not be forthcoming by the free volume approach used in the past to capture molecular dynamics of the entire softening dispersion. It remains to be seen if comparable levels of understanding can be reached in polysaccharide networks, which exhibit distinct topology from that of gelatin in mixture with small polyhydroxyl compounds.

References and Notes

- (1) Huang, Y.; Paul, D. R. *Polymer* **2004**, *45*, 8377.
- (2) Fox, T. G., Jr.; Flory, P. J. *J. Appl. Phys.* **1950**, *21*, 581.
- (3) Li, X.; Yee, A. F. *Macromolecules* **2003**, *36*, 9411.
- (4) Slade, L.; Levine, H. In *Advances in Food and Nutrition Research*; Kinsella, J. E., Taylor, S. L., Eds.; Academic Press: San Diego, 1995; p 103.
- (5) Blachot, J.-F.; Chazeau, L.; Cavaille, J.-Y. *Polymer* **2002**, *43*, 881.
- (6) Slade, L.; Franks, F. In *Amorphous Food and Pharmaceutical Systems*; Levine, H. Ed.; The Royal Society of Chemistry: Cambridge, UK, 2002; p x.
- (7) Dlubek, G.; Buchhold, R.; Hubner, Ch.; Nakladal, A. *Macromolecules* **1999**, *32*, 2348.
- (8) Ferry, J. D. *Macromolecules* **1991**, *16*, 5237.
- (9) Matsuoka, S. *Polym. Eng. Sci.* **1981**, *21*, 907.
- (10) Li, H.-L.; Ujihira, Y.; Nanasawa, A. *J. Radioanal. Nucl. Chem.* **1996**, *210*, 533.
- (11) Alves, N. M.; Mano, J. F.; Gomez Ribelles, J. L.; Gomez Tejedor, J. A. *Polymer* **2004**, *45*, 1007.
- (12) Kasapis, S.; Al-Marhoobi, I. M. *Biomacromolecules* **2005**, *6*, 14.
- (13) Ngai, K. L.; Plazek, D. J. *Rubber Chem. Technol.* **1995**, *68*, 376.
- (14) Hutchinson, J. M. *Prog. Polym. Sci.* **1995**, *20*, 703.
- (15) Ngai, K. L. *J. Non-Cryst. Solids* **2000**, *275*, 7.
- (16) Ngai, K. L.; Roland, C. M. *Polymer* **2002**, *43*, 567.
- (17) Evangelou, V.; Kasapis, S.; Hember, M. W. N. *Polymer* **1998**, *39*, 3909.
- (18) Ward, I. M.; Hadley, D. W. In *An Introduction to the Mechanical Properties of Solid Polymers*; Wiley: Chichester, U.K., 1993; p 45.
- (19) Kasapis, S.; Desbrières, J.; Al-Marhoobi, I. M.; Rinaudo, M. *Carbohydr. Res.* **2002**, *337*, 595.
- (20) Kasapis, S.; Morris, E. R.; Norton, I. T.; Clark, A. H. *Carbohydr. Polym.* **1993**, *21*, 243.
- (21) Kasapis, S.; Mitchell, J.; Abeysekera, R.; MacNaughtan, W. *Trends Food Sci. Technol.* **2004**, *15*, 298.
- (22) Normand, V.; Muller, S.; Ravey J.-C.; Parker, A. *Macromolecules* **2000**, *33*, 1063.
- (23) Guo, L.; Colby, R. H.; Lusignan, C. P.; Whitesides, T. H. *Macromolecules* **2003**, *36*, 9999.
- (24) Ecker, C.; Severin, N.; Shu, L.; Schluter, A. D.; Rabe, J. P. *Macromolecules* **2004**, *37*, 2484.
- (25) Tsoga, A.; Kasapis, S.; Richardson, R. K. *Biopolymers* **1999**, *49*, 267.
- (26) Roos, Y. H. In *Phase Transitions in Foods*; Academic Press: San Diego, 1995; p 116.
- (27) Roland, C. M.; Santangelo, P. G.; Ngai, K. L.; Meier, G. *Macromolecules* **1993**, *26*, 6164.
- (28) Normand, V.; Aymard, P.; Lootens, D. L.; Amici, E.; Plucknett, K. P.; Frith, W. J. *Carbohydr. Polym.* **2003**, *54*, 83.
- (29) Van Melick, H. G. H.; Govaert, L. E.; Meijer, H. E. H. *Polymer* **2003**, *44*, 2493.
- (30) Ferry, J. D. In *Viscoelastic Properties of Polymers*; Wiley: New York, 1980; p 68.
- (31) Ferry, J. D. *J. Am. Chem. Soc.* **1950**, *72*, 3746.
- (32) Lazaridou, A.; Biliaderis, C. G. *Carbohydr. Polym.* **2002**, *48*, 179.
- (33) Ferry, J. D. In *Viscoelastic Properties of Polymers*; Wiley: New York, 1980; p 264.

- (34) Freitas, R. A.; Martin, S.; Paula, R. C.; Feitosa, J. P. A.; Sierakowski, M.-R. *Thermochim. Acta* **2004**, 409, 41.
- (35) Williams, M. L.; Landel, R. F.; Ferry, J. D. *J. Am. Chem. Soc.* **1955**, 77, 3701.
- (36) Rieger, J. *Polym. Test.* **2001**, 20, 199.
- (37) Peleg, M. *Rheol. Acta* **1995**, 34, 215.
- (38) Marshall, A. S.; Petrie, S. E. B. *J. Photogr. Sci.* **1980**, 28, 128.
- (39) Kasapis, S.; Al-Marhoobi, I. M.; Mitchell, J. R. *Carbohydr. Res.* **2003**, 338, 787.
- (40) Arridge, R. G. C. In *Mechanics of Polymers*; Clarendon Press: Oxford, U.K., 1975; p 24.
- (41) Plazek, D. J. *J. Rheol.* **1996**, 40, 987.
- (42) Nandan, B.; Kandpal, L. D.; Mathur, G. N. *Polymer* **2003**, 44, 1267.
- (43) Tchesskaya, T. Yu. *J. Mol. Liq.* **2005**, 120, 143.
- (44) Tobolsky, A. V.; Akonis, J. J. *J. Phys. Chem.* **1964**, 68, 1970.
- (45) Yano, T.; Nagano, T.; Lee, J.; Shibata, S.; Yamane, M. *Solid State Ionics* **2002**, 150, 281.
- (46) Williams, G.; Watts, D. C. *Trans. Faraday Soc.* **1970**, 66, 80.
- (47) Ngai, K. L.; Yee, A. F. *J. Polym. Sci., Part B: Polym. Phys.* **1991**, 29, 1493.
- (48) Kasapis, S.; Al-Marhoobi, I. M.; Deszczynski, M.; Mitchell, J. R.; Abeysekera, R. *Biomacromolecules* **2003**, 4, 1142.
- (49) Roland, C. M.; Ngai, K. L. *Macromolecules* **1991**, 24, 5315.
- (50) Kasapis, S.; Al-Marhoobi, I. M.; Mitchell, J. R. *Biopolymers* **2003**, 70, 169.
- (51) Frick, F.; Zorn, R.; Richter, D.; Farago, B. *J. Non-Cryst. Solids* **1991**, 131–133, 169.
- (52) Kasapis, S. *Food Hydrocolloids* **2006**, 20, 218.

BM060189S